# Location of Transmission Line faults using Radial Basis Function based Artificial Neural Networks

Rabindra N. Mahanty and P. B. Dutta Gupta

*Abstract*--**A scheme for location of transmission line faults based on Radial Basis Function based Artificial Neural Networks is presented. Post-fault current and voltage samples are considered as inputs to ANNs. To validate the proposed scheme simulation studies have been carried out using EMTP and MATLAB on a power system model considering wide variations in fault inception angle, fault location and fault resistance.**

***Index Terms*-- Fault location, transmission line, Radial Basis Function, Neural Network.**

## I. INTRODUCTION

TRANSMISSION lines are vital links in a power system, which provide the essential continuity of service from generating plants to the end users. Fast and accurate detection and classification of transmission line faults are required in order to maintain a reliable power system operation. Accurate location of the fault point is necessary to ensure quick service restoration.

Two types of algorithms, the differential equation based algorithms [1-5] and the Fourier analysis based algorithms [1,6,7] are widely accepted for transmission line fault location. However, both types of algorithms are affected by the presence of fault resistance ($R_F$). Travelling wave based algorithms are also capable of accurately locating faults but implementation of these schemes becomes complicated because of difficulty in accurate detection of signals.

The multilayer feedforward network with back propagation (BP) training algorithm is the most widely used neural network model for pattern classification applications [8]. However, BP is not well suited for distance protection as the algorithm does not work satisfactorily when a case to be diagnosed falls in a region with no training data. The radial basis function (RBF) based neural network is well suited for such cases [9,10].

A RBF neural network based fault location scheme is presented. Large number of patterns has been generated by means of EMTP. Some of these have been used for training and some have been used for testing. Simulation studies have been carried out on a power system model, considering wide variations in fault inception angle, fault location and fault resistance.

Rabindra N. Mahanty is with the Electrical Engineering Department, Indian Institute of Technology, Kharagpur-721302, India, on leave from Regional Institute of Technology, Jamshedpur-831014, India, for pursuing Ph. D. degree (e-mail: mahantyr@ee.iitkgp.ernet.in ).
P. B. Dutta Gupta is with the Electrical Engineering Department, Indian Institute of Technology, Kharagpur-721302, India (telephone: 03222-83050, e-mail: pbdg@ee.iitkgp.ernet.in ).

## II. R B F NEURAL NETWORK

The radial basis function network (RBFN) has a feedforward structure consisting of three layers, an input layer, a nonlinear hidden layer and a linear output layer, as shown in Fig. 1. The hidden nodes are the radial basis function units and the output nodes are simple summations. The number of input, output and hidden nodes are $n_I$, $n_o$ and $n_h$ respectively. This particular architecture of RBFN has proved to directly improve training and performance of the network [9]. Any of the functions viz. spline, multiquadratic, Gaussian function may be used as transfer function for the hidden neurons. The Gaussian RBF, which is the most widely used one, has been considered for the proposed fault location application.

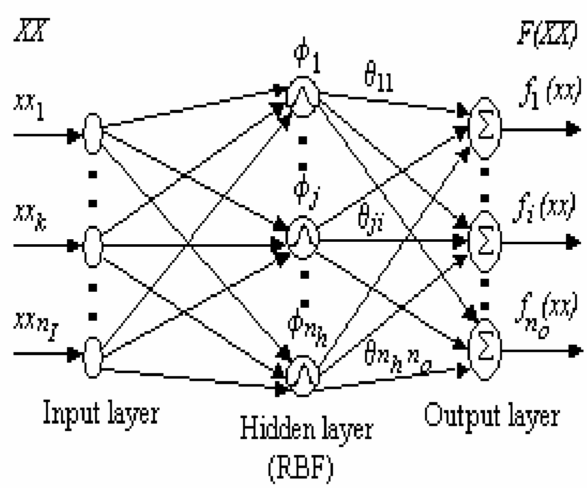


**Fig. 1** Architecture of RBF neural network

The response of the $j^{th}$ hidden neuron to the input $xx_k$ is expressed as [10]:

$$\phi_j(xx_k) = exp\left(-\frac{1}{\sigma_j^2}\left\| xx_k - \mu_j \right\|^2\right) \qquad (1)$$

where $\mu_j$ is the center for the $j^{th}$ hidden neuron and $\sigma_j$ is the spread of the Gaussian function, $\| \ \|$ denotes the Euclidian norm. The output of each node in the output layer is defined by [10]

$$f_i(\boldsymbol{XX}) = \sum_{j=1}^{n_h} \phi_j\,(\boldsymbol{XX}\text{-}\mu_j)\,\theta_{ji} \qquad (2)$$

where $\boldsymbol{XX}$ is the input vector and $\theta_{ji}$ represents the weight from the $j^{th}$ hidden node to the $i^{th}$ output node.

The performance of a RBF neural network depends on the choice of the values of the centers. In the proposed work, the simulation studies have been carried out by means of MATLAB's "neural network toolbox" [14], which makes use of the orthogonal least squares (OLS) learning procedure [11,12] for determining the RBF centers.

## III. Power System Model

The power system model considered for simulation study is shown in Figure 2. As shown in the figure fault occurs on transmission line 1.

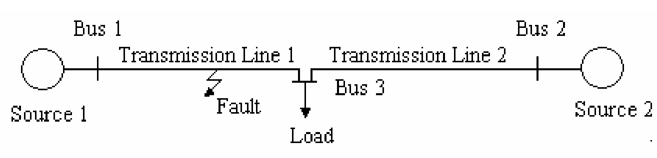


**Fig. 2** : A faulted transmission line fed from both ends

The line parameters and other relevant data are as shown below.

<u>Transmission line 1</u>

Line length = 100Km
Positive sequence line parameters: $R$ = 2.34 Ω, $L$ = 95.10 mH, $C$ = 1.24 μF.
Zero sequence line parameters: $R$ = 38.85 Ω, $L$ = 325.08 mH, $C$ = 0.845 μF.

<u>Transmission line 2</u>

Line length = 130 km
$R_2$ =1.3 $R_1$, $L_2$ =1.3 $L_1$, $C_2$ =$C_1$, where suffixes 1 and 2 refer to transmission line-1 and transmission line-2 respectively.
$v_{S1}$= 400 kV, $v_{S2}$ = 0.95 $v_{S1}$, where $v_{S1}$and $v_{S2}$ are the voltages of source 1 and source 2.
$\delta$ (phase difference between $v_{S1}$ and $v_{S2}$ )=20$^0$ with $v_{S1}$ leading.
Source impedances: $Z_{S1}$ = (0.2 + j4.5) Ω per phase, $Z_{S2}$ = (0.3 + j8) Ω per phase.

## IV. The Fault Locator

The proposed ANN based fault locator is shown in Fig. 3. As shown in the figure, the proposed fault locator consists of two ANNs: ANN-I and ANN-II for each type of fault *i. e.* two ANNs for *L-G* faults, two ANNs for *L-L* faults and so on. The two ANNs are trained with different values of spread. The operating principle of the fault locator is as follows. After the type of fault has been identified, ANN-I assigned for the particular type of fault estimates the fault location. In case this estimate is less than a specified predetermined value (corresponding to 50% of line length) then a second estimate is found out using ANN-II for the type of fault. In case the first estimate is equal to or greater than the specified value, then there is no need to find second estimate. The training and testing data are generated using EMTP [13] considering a sampling interval of 1ms. The fault location is carried out by a MATLAB program, which makes use of the 'Neural Network Toolbox' [14]. The prerequisite of the fault location program is that the fault type should be known. There are several established methods by which this can be done [8,9,10].

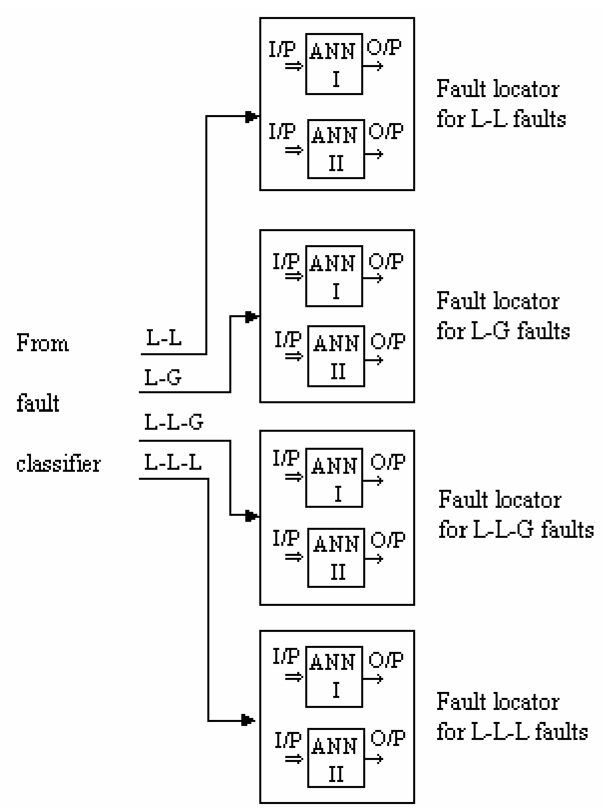


**Fig. 3** The proposed ANN based fault locator

## V. Simulation Study

The input to each ANN consists of ten post-fault samples of each of the three phase currents and voltages, taken at one end of line (bus 1 of Fig. 2). The input data are all normalized and are presented in the form of a single input vector to ANN. Corresponding to the input vector an output is obtained in terms of fraction of the line length up to the fault point.

In order to achieve high degree of accuracy in fault location, large number of training data have been generated using EMTP, considering fault at 10%, 20%, 30%……60%,70%, 75%, 80%, 85% and 90% of the line. For each fault location, fault inception angles of $0^0$, $20^0$, $40^0$, $60^0$ and $80^0$ and fault resistances of 0.5Ω, 20Ω, 75Ω and 150Ω have been considered. A per phase load impedance of 500Ω at 0.8 p. f. lagging has been considered for all training cases.

After carrying out a number of simulation studies, it has been observed that instead of a single value of spread for the entire line if two different values of spread are used, one for faults within about 50% of line and another for faults beyond this range, more accurate estimates of fault location are obtained. The above mentioned strategy of estimating fault location is implemented by using two ANNs: ANN-I ( for faults occurring beyond 50% of line) and ANN-II ( for faults occurring within 50% of line) for each type of fault, the two ANNs being trained with different values of spread. The selected values of the spreads for various ANNs for location of L-L and L-G faults are shown in Table I. The number of neurons in the hidden layer, the number of epochs (iterations) and the training time of each ANN are also shown in these

TABLE I
SPREADS RELATING TO VARIOUS ANNS OF FAULT LOCATOR

| Fault type | Network | Optimal Spread | Epochs | Number of hidden neurons | Training time (mins) |
|---|---|---|---|---|---|
| L-L | ANN-I | 1.6 | 181 | 181 | 4.62 |
| | ANN-II | 0.8 | 193 | 193 | 5.06 |
| L-G | ANN-I | 1.0 | 163 | 163 | 3.98 |
| | ANN-II | 1.6 | 175 | 175 | 4.46 |

tables. The error goal was fixed at 0.001 for all ANNs. The error convergence of the various ANNs used for locating L-G and L-L faults are shown in Fig. 4 through Fig. 7.

After the training phase was over, each ANN was tested for different types of faults considering wide variations in fault

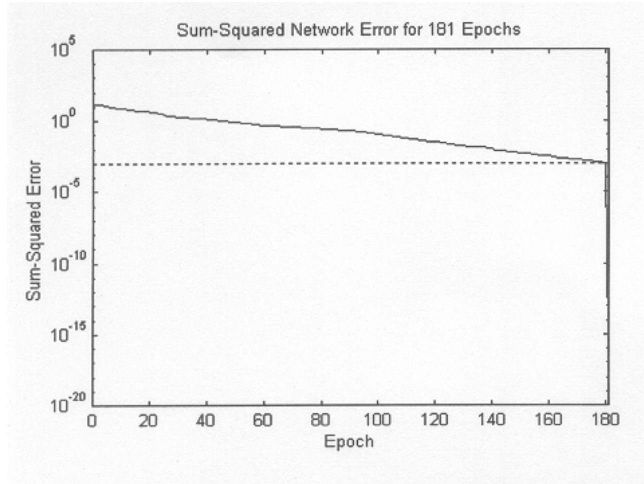


Fig. 4 Error convergence of ANN-I for L-L faults in training

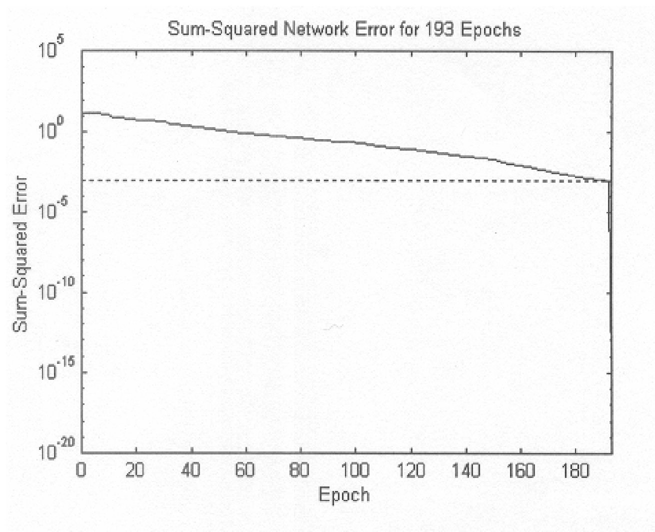


Fig. 5 Error convergence of ANN-II for L-L faults in training

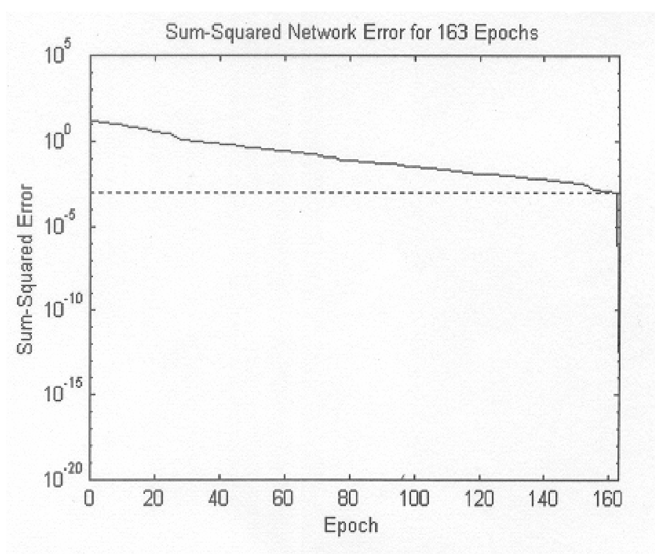


Fig. 6 Error convergence of ANN-I for L-G faults in training

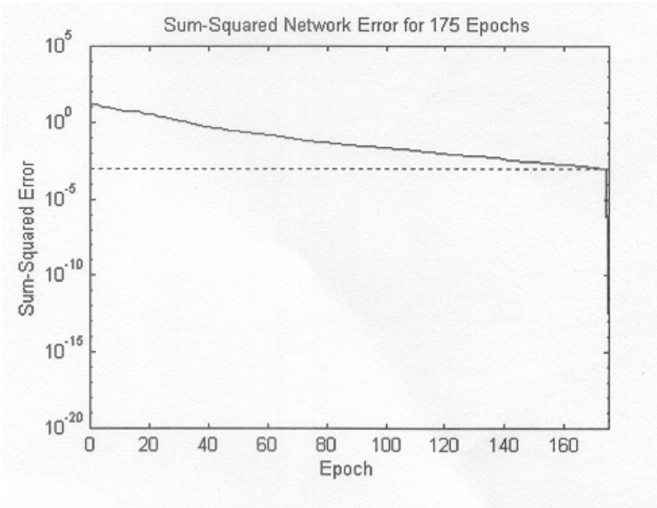


Fig. 7 Error convergence of ANN-II for L-G faults in training

location, fault resistances, fault inception angle and pre-fault load. A variation of 0-200Ω in fault resistance ($R_F$), 0-360$^0$ in fault inception angle (*FIA*) and 0-90% of transmission line length in fault location ($\alpha$) have been considered. The above variations were combined with a per phase load ($Z_L$) variation of 300-1200Ω with variation of 0.7–0.9 in power factor (lagging). A comparison of results obtained with the two selected values of spread are shown in Table II. $\alpha_e$ represents the estimate of fault location obtained through ANN.As shown in Table II, for *L-L/L-G* faults at 15% of line, results obtained with ANN-II are generally better than those obtained with ANN-I. Similarly, for *L-L/L-G* faults at 82% of, the results obtained with ANN-I are generally more accurate. The other results shown in Tables II also depict the fact that the use of two values of spread is justified.

Some representative test results are presented in Table III and Table IV, which confirm the feasibility of the proposed ANN based fault location scheme.

TABLE II

COMPARISON OF FAULT LOCATION ESTIMATES FOR THE TWO SELECTED VALUES OF SPREAD

| Fault type | $\alpha$ | $Z_L$ (Ω) | $R_F$ (Ω) | FIA (°) | Network | $\alpha_e$ |
|---|---|---|---|---|---|---|
| A-G | 0.15 | 400∠36.87° | 0.01 | 0 | ANN-I | 0.1381 |
| | | | | | ANN-II | 0.1466 |
| | | | | 90 | ANN-I | 0.1496 |
| | | | | | ANN-II | 0.1521 |
| | | 1200∠45.57° | 200 | 0 | ANN-I | 0.1420 |
| | | | | | ANN-II | 0.1509 |
| | | | | 90 | ANN-I | 0.1376 |
| | | | | | ANN-II | 0.1579 |
| | 0.82 | 400∠36.87° | 0.01 | 0 | ANN-I | 0.8142 |
| | | | | | ANN-II | 0.8081 |
| | | | | 90 | ANN-I | 0.7889 |
| | | | | | ANN-II | 0.8740 |
| | | 1200∠45.57° | 200 | 0 | ANN-I | 0.8146 |
| | | | | | ANN-II | 0.8168 |
| | | | | 90 | ANN-I | 0.7966 |
| | | | | | ANN-II | 0.7892 |
| A-B | 0.15 | 400∠36.87° | 0.01 | 0 | ANN-I | 0.1266 |
| | | | | | ANN-II | 0.1381 |
| | | | | 90 | ANN-I | 0.1318 |
| | | | | | ANN-II | 0.1276 |
| | | 1200∠45.57° | 200 | 0 | ANN-I | 0.1779 |
| | | | | | ANN-II | 0.1650 |
| | | | | 90 | ANN-I | 0.1699 |
| | | | | | ANN-II | 0.1549 |
| | 0.82 | 400∠36.87° | 0.01 | 0 | ANN-I | 0.8192 |
| | | | | | ANN-II | 0.8103 |
| | | | | 90 | ANN-I | 0.8183 |
| | | | | | ANN-II | 0.8096 |
| | | 1200∠45.57° | 200 | 0 | ANN-I | 0.7946 |
| | | | | | ANN-II | 0.7711 |
| | | | | 90 | ANN-I | 0.7978 |
| | | | | | ANN-II | 0.7375 |

## VI. CONCLUSION

A Methodology for location of transmission line faults based on RBF neural network have been presented. Samples of three phase voltages and currents are used as inputs to the ANNs of the fault locator. In order to obtain accurate estimates, two ANNs with different values of spread have been used for each type of fault. Simulation studies carried out considering wide variations in fault location, fault inception angle, fault resistance and pre-fault load, show that the proposed methods are suitable for location of transmission line faults including the high impedance ones.

TABLE III

TEST RESULTS FOR **AG** FAULT AT 15% OF LINE

| $R_F$ ($\Omega$) | $Z_L$ ($\Omega$) | FIA ($^0$) | $\alpha_e$ |
|---|---|---|---|
| | | 0 | 0.1466 |
| | | 15 | 0.1171 |
| 0 | $400\angle 36.87^0$ | 45 | 0.1233 |
| | | 75 | 0.1398 |
| | | 90 | 0.1521 |
| | | 0 | 0.1902 |
| | | 15 | 0.1594 |
| 10 | $1200\angle 45.57^0$ | 45 | 0.1212 |
| | | 75 | 0.1606 |
| | | 90 | 0.1917 |
| | | 0 | 0.1506 |
| | | 15 | 0.1840 |
| 50 | $800\angle 45.57^0$ | 45 | 0.1531 |
| | | 75 | 0.1842 |
| | | 90 | 0.1567 |
| | | 0 | 0.1509 |
| | | 15 | 0.1744 |
| 200 | $1200\angle 45.57^0$ | 45 | 0.1396 |
| | | 75 | 0.2006 |
| | | 90 | 0.1579 |

## VII. REFERENCES


[1] A. G. Phadke and J. S. Thorp, "Computer Relaying for Power Systems", Research Studies Press Ltd., Taunton, England, 1988.

[2] W. D. Breingan and M. M. Chen. "The laboratory investigation of a digital system for the protection of transmission lines", *IEEE Trans. Power Apparatus and Systems.* Vol. 98. No. 2, pp. 350-368,1979.

[3] W. J. Smolinski, "An algorithm for digital impedance calculation using a single pi section transmission line model", *IEEE Trans. Power Apparatus and System,* Vol. 98, No. 5, pp. 1546-1551, 1979.

[4] A. M. Ranjbar and B. J. Cory, "An improved method for the digital protection of high voltage transmission lines", *IEEE Trans. Power Apparatus and Systems,* Vol. 94, No. 2, pp. 544-550, 1975.

[5] M. Akke and J. T. Thorp, "Some improvements in the three phase differential equation for fast transmission line protection", *IEEE Trans. Power Delivery.* Vol. 13, No. 1, pp. 66-72 ,1998.

[6] M. Ramamoorty, "Application of digital computers to power system protection," *Journal of Institution of Engineers, India*, Vol. 52, No. 10, pp. 235-238, 1972.

[7] A. Wiszniewski, "Accurate fault impedance locating algorithm", *IEE Proc. C. Generation, Transmission and Distribution*, Vol. 130, No. 6, pp. 311-314,1983.

[8] F. Zahra, B. Jeyasurya and J. E. Quaicoe, "High speed transmission line relaying using artificial neural networks", *Electric Power Systems Research*, Vol. 53, pp. 173-179, 2000.

[9] Y. H. Song, Q. Y. Xuan and A. T. Johns, "Protection scheme for E H V transmission systems with thyristor controlled series compensation using radial basis function neural networks," *Electric Machines and Power Systems*, Vol. 25, pp. 553-565,1997.

[10] P. K. Dash, A. K. Pradhan and G. Panda, "Application of minimal radial basis function neural network to distance protection", *IEEE Trans. Power Delivery*, Vol.16, No.1, pp. 68-74 , 2000.

[11] S. Chen, C. F. N. Cowan and P. M. Grant, "Orthogonal least squares learning algorithm for radial basis function networks", *IEEE Trans. Neural Networks*, Vol. 2, No. 2, pp. 302-309, 1991.

[12] S. Chen, P. M. Grant and C. F. N. Cowan, "Orthogonal least squares algorithm for training multioutput radial basis function networks", *IEE Proc. Neural Networks*, Vol. 139, No. 6, pp. 378-384, 1992.

[13] Microtran Reference Manual., "Transients analysis program for power and power electronic circuits", Microtran power system analysis corporation. Vancouver, Canada (1997).

[14] H. Demuth and M. Beale, "Neural network toolbox for use with Matlab", The Mathworks, Inc., USA, 1996.


TABLE IV

TEST RESULTS FOR **AB** FAULT AT 55% OF LINE

| $R_F$ ($\Omega$) | $Z_L$ ($\Omega$) | FIA ($^0$) | $\alpha_e$ |
|---|---|---|---|
| | | 0 | 0.5482 |
| | | 15 | 0.4941 |
| 0 | $400\angle 36.87^0$ | 45 | 0.5469 |
| | | 75 | 0.5157 |
| | | 90 | 0.5468 |
| | | 0 | 0.5500 |
| | | 15 | 0.5586 |
| 10 | $1200\angle 45.57^0$ | 45 | 0.5530 |
| | | 75 | 0.5392 |
| | | 90 | 0.5501 |
| | | 0 | 0.4943 |
| | | 15 | 0.5310 |
| 50 | $800\angle 45.57^0$ | 45 | 0.5550 |
| | | 75 | 0.5416 |
| | | 90 | 0.4863 |
| | | 0 | 0.5323 |
| | | 15 | 0.5665 |
| 200 | $1200\angle 45.57^0$ | 45 | 0.5956 |
| | | 75 | 0.6085 |
| | | 90 | 0.5523 |